Field-theoretic approach to the universality of branching processes

Rosalba Garcia-Millan,[*] Johannes Pausch,[†] Benjamin Walter,[‡] and Gunnar Pruessner[§]

Department of Mathematics, Imperial College London, London SW7 2AZ, United Kingdom

Branching processes are widely used to model phenomena from networks to neuronal avalanching. In a large class of continuous-time branching processes, we study the temporal scaling of the moments of the instant population size, the survival probability, expected avalanche duration, the so-called avalanche shape, the n-point correlation function, and the probability density function of the total avalanche size. Previous studies have shown universality in certain observables of branching processes using probabilistic arguments; however, a comprehensive description is lacking. We derive the field theory that describes the process and demonstrate how to use it to calculate the relevant observables and their scaling to leading order in time, revealing the universality of the moments of the population size. Our results explain why the first and second moment of the offspring distribution are sufficient to fully characterize the process in the vicinity of criticality, regardless of the underlying offspring distribution. This finding implies that branching processes are universal. We illustrate our analytical results with computer simulations.

I. INTRODUCTION

Branching processes [1] are widely used for modeling phenomena in many different subject areas, such as avalanches [2–4], networks [3–6], earthquakes [7,8], family names [9], populations of bacteria and cells [10,11], nuclear reactions [12,13], cultural evolution [14], and neuronal avalanches [15,16]. Because of their mathematical simplicity they play an important role in statistical mechanics [17] and the theory of complex systems [8].

Branching processes are a paradigmatic example of a system displaying a second-order phase transition between extinction (absorbing state) with probability one and nonzero probability of survival (nonabsorbing state) in the infinite time limit. The critical point in the parameter region at which this transition occurs is where branching and extinction rates exactly balance, namely when the expected number of offspring per particle is exactly unity [1,8].

In the present work we study the continuous-time version of the Galton-Watson branching process [1], which is a generalization of the birth-death process [18,19]. In the continuous-time branching process, particles go extinct or replicate into a number of identical offspring at random and with constant Poissonian rates. Each of the new particles follows the same process. The difference between the original Galton-Watson branching process and the continuous-time branching process we consider here, lies in the waiting times between events. In the original Galton-Watson branching process, updates occur in discrete time steps, while in the continuous-time process we consider, waiting times follow a Poisson process [18,19]. However, both processes share many asymptotics [1,17], and therefore we regard the continuous-time branching process as the continuum limit of the Galton-Watson branching process.

By using field-theoretic methods, we provide a general framework to determine universal, finite-time scaling properties of a wide range of branching processes close to the critical point. The main advantages of this versatile approach are, on the one hand, the ease with which observables are calculated and, on the other hand, the use of diagrammatic language, which allows us to manipulate the sometimes cumbersome expressions in a neat and compact way. Other methods in the literature developed to study problems related to branching processes, in particular relating branching processes to different forms of motion, include the formalism based on the Pal-Bell equation [20–22].

Moreover, our framework allows us to determine systematically observables that are otherwise complicated to manipulate if possible at all. To illustrate this point, we have calculated in closed form a number of observables that describe different aspects of the process in the vicinity of the critical point: we have calculated the moments of the population size as a function of time, the probability distribution of the population size as a function of time, the avalanche shape, the two-time and n-time correlation functions, and the total avalanche size and its moments.

Our results show that branching processes are universal in the vicinity of the critical point [23,24] in the sense that exactly three quantities (the Poissonian rate and the first and second moments of the offspring distribution) are sufficient to describe the asymptotics of the process regardless of the underlying offspring distribution.

The contents of this paper are organised as follows. In Sec. II we derive the field theory of the continuous-time branching process. In Sec. III we use our formalism to calculate a number of observables in closed form, and in Sec. IV we discuss our results and our conclusions. Further details of the calculations can be found in the Appendices.

———————
[*]garciamillan16@imperial.ac.uk
[†]j.pausch15@imperial.ac.uk
[‡]b.walter16@imperial.ac.uk
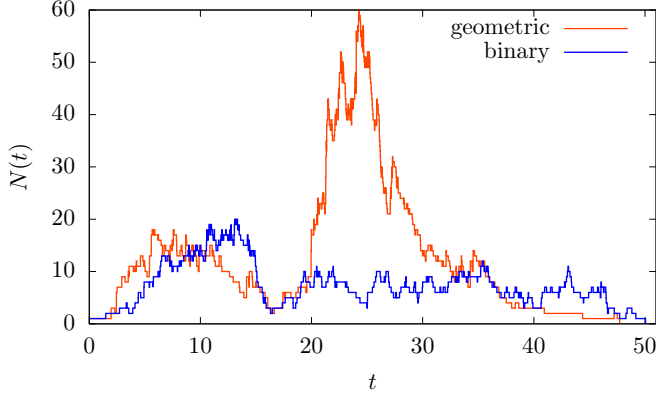[§]g.pruessner@imperial.ac.uk

FIG. 1. Typical avalanche profiles $N(t)$ of a binary branching process (blue) and a branching process with geometric distribution of the number of offspring (orange), both at criticality $r = 0$ and with Poissonian rate $s = 1$.

II. FIELD THEORY OF THE CONTINUOUS-TIME BRANCHING PROCESS

The continuous-time branching process is defined as follows. We consider a population of $N(t)$ identical particles at time $t \geqslant 0$ with initial condition $N(0) = 1$. Each particle is allowed to branch independently into κ offspring with Poissonian rate $s > 0$, where $\kappa \in \{0\} \cup \mathbb{N}$ is a random variable with probability distribution $P(\kappa = k) = p_k \in [0, 1]$ [18], Fig. 1. In the language of chemical reactions, this can be written as the reaction $A \to \kappa A$.

To derive the field theory of this process following the methods by Doi and Peliti [17,25–27], we first write the master equation of the probability $P(N, t)$ to find N particles at time t,

$$\frac{dP(N, t)}{dt} = s \sum_k p_k(N - k + 1)P(N - k + 1, t) - sNP(N, t), \tag{1}$$

with initial condition $P(N, 0) = \delta_{N,1}$. Following work by Doi [25], we cast the master equation in a second quantized form. A system with N particles is represented by a Fock-space vector $|N\rangle$. We use the ladder operators $a^\dagger$ (creation) and a (annihilation), which act on $|N\rangle$ such that $a|N\rangle = N|N - 1\rangle$ and $a^\dagger|N\rangle = |N + 1\rangle$, and satisfy the commutation relation $[a, a^\dagger] = aa^\dagger - a^\dagger a = 1$. The probabilistic state of the system is given by

$$|\Psi(t)\rangle = \sum_N P(N, t)|N\rangle, \tag{2}$$

and its time evolution is determined by Eq. (1),

$$\frac{d|\Psi(t)\rangle}{dt} = s(f(a^\dagger) - a^\dagger)a|\Psi(t)\rangle, \tag{3}$$

using the probability generating function of κ,

$$f(z) = \sum_{k=0}^\infty p_k z^k = \langle z^\kappa \rangle, \tag{4}$$

where $\langle \bullet \rangle$ denotes expectation. We define the *mass r* as the difference between the extinction and the net branching rates,

$$r = sp_0 - s \sum_{k \geqslant 2}(k - 1)p_k = s(1 - \langle \kappa \rangle), \tag{5}$$

and the rates q_j as

$$q_j = s \sum_k \binom{k}{j} p_k = s \left\langle \binom{\kappa}{j} \right\rangle = \frac{s}{j!} f^{(j)}(1), \tag{6}$$

where $f^{(j)}(1)$ denotes the jth derivative of the probability generating function Eq. (4) evaluated at $z = 1$. We assume that the rates q_j are finite. In this notation, the time evolution in Eq. (3) can be written as

$$\tilde{\mathcal{A}}|\Psi(t)\rangle = \frac{d}{dt}|\Psi(t)\rangle \quad \text{and thus} \quad |\Psi(t)\rangle = e^{\tilde{\mathcal{A}}t}|\Psi(0)\rangle, \tag{7}$$

where $\tilde{\mathcal{A}}$ is the operator

$$\tilde{\mathcal{A}} = \sum_{j \geqslant 2} q_j \widetilde{a}^j a - r\widetilde{a}a, \tag{8}$$

and $\widetilde{a}$ denotes the Doi-shifted creation operator, $a^\dagger = 1 + \widetilde{a}$.

The sign of the mass r, Eq. (5), determines in which regime a particular branching process is in: if $r = 0$, then the process is at the critical point: if $r > 0$, then the process is in the subcritical regime; and if $r < 0$, then the process is in the supercritical regime. Subcritical and critical processes are bound to go extinct in finite time, whereas supercritical process have a positive probability of survival [1].

Following the work by Peliti [26], Eq. (3) can be cast in path integral form. Here, the creation and annihilation operators $a^\dagger$ and a are transformed to time-dependent creation and annihilation fields $\phi^\dagger(t)$ and $\phi(t)$ respectively. Similarly, the Doi-shifted operator $\widetilde{a}$ is transformed to the time-dependent Doi-shifted field $\widetilde{\phi}(t) = \phi^\dagger(t) - 1$. The action functional of the resulting field theory is given by

$$\mathcal{A}[\widetilde{\phi}, \phi] = \int_{-\infty}^\infty dt \left\{ \sum_{j \geqslant 2} q_j \widetilde{\phi}^j(t)\phi(t) - \widetilde{\phi}(t)\left(\frac{d}{dt} + r\right)\phi(t) \right\}. \tag{9}$$

Using the Fourier transform

$$\phi(t) = \int \dbar\omega \, \phi(\omega)e^{-\hat{i}\omega t} \quad \text{with} \quad \dbar\omega = \frac{d\omega}{2\pi}, \tag{10a}$$

$$\phi(\omega) = \int dt \, \phi(t)e^{\hat{i}\omega t}, \tag{10b}$$

and identically for $\widetilde{\phi}(t)$, the action Eq. (9) becomes local in ω and the bilinear, i.e., the Gaussian part,

$$\mathcal{A}_0[\widetilde{\phi}, \phi] = -\int \dbar\omega \, \widetilde{\phi}(-\omega)(-\hat{i}\omega + r)\phi(\omega), \tag{11}$$

of the path integral can be determined in closed form. The Gaussian path integral is well-defined only when the mass is positive, $r > 0$. The nonlinear terms, $j \geqslant 2$ in Eq. (9), are then treated as a perturbation about the Gaussian part, as commonly done in field theory [17,28].

TABLE I. Summary of observables including their equation number and what cases and limits are Exact. The expressions referred to are, in the limit $r \to 0$, either: *exact*, *exact for binary branching processes* (i.e., for other branching process, our result is the leading order in q_2/r for small r at fixed rt), or provide *exact asymptotes* (that is, our result is the leading order for any kind of branching process). The regime of validity near criticality is either critical and subcritical ($r \geqslant 0$) or all encompassing ($r \in \mathbb{R}$).

Observable	Symbol	Equations	Expression	Regime	Figure
Moments of the number of particles $N(t)$	$\langle N^n(t) \rangle$	(35), (36)	Exact asymptote	$r \in \mathbb{R}$	2
Moments of the number of particles $N(t)$	$\langle N^n(t) \rangle, n \in \{1, 2, 3\}$	(A1)	Exact	$r \in \mathbb{R}$	2
Moment generating function of $N(t)$	$\mathcal{M}_N(z)$	(38)	Exact asymptote	$r \in \mathbb{R}$	
Probability distribution of $N(t)$	$P(N, t)$	(41)	Exact for binary bp	$r \in \mathbb{R}$	
Probability of survival	$P_s(t)$	(42), (43)	Exact for binary bp	$r \in \mathbb{R}$	3
Distribution of the avalanche duration T	$\mathcal{P}_T(t)$	(44), (45)	Exact for binary bp	$r \geqslant 0$	
Expected avalanche duration	$\langle T \rangle$	(46)	Exact for binary bp	$r \geqslant 0$	4
Avalanche shape	$V(t, T)$	(52), (53)	Exact for binary bp	$r \in \mathbb{R}$	5(a)
Averaged avalanche shape	$\langle V(\tau) \rangle_T$	(C2)	Exact for binary bp	$r \in \mathbb{R}$	5(b)
Two-point connected correlation function	$\text{Cov}(N(t_1), N(t_2))$	(56)	Exact	$r \in \mathbb{R}$	6
Three-point correlation function	$\langle N(t_1)N(t_2)N(t_3) \rangle$	(A3)	Exact	$r \in \mathbb{R}$	
Moments of the total avalanche size S	$\langle S^n \rangle$	(59), (60)	Exact asymptote	$r \geqslant 0$	
Moment generating function of S	$\mathcal{M}_S(z)$	(62)	Exact asymptote	$r \geqslant 0$	
Distribution of S	$\mathcal{P}_S(x)$	(63)	Exact asymptote	$r \geqslant 0$	7

III. OBSERVABLES

We use the field theory described above to calculate a number of observables that have received attention in the literature in various settings. In Table I we list all the observables that we have calculated in closed form and the degree of approximation of our analytical result. Some results are exact for any kind of branching process and other results are only exact for binary branching processes. Those results that are an approximation have the exact asymptotic ehavior.

All observables are constructed on the basis of the probability vector $|\Psi(t)\rangle$ which evolves according to Eq. (7). If the initial state, $t = 0$, consists of a single particle, then $|\Psi(0)\rangle = a^\dagger|0\rangle$ and $|\Psi(t)\rangle = \exp(\tilde{\mathcal{A}}t)a^\dagger|0\rangle$. Probing the particle number requires the action of the operator $a^\dagger a$, whose eigenvectors are the pure states $|N\rangle$, such that $a^\dagger a|N\rangle = N|N\rangle$. The components of the vector $a^\dagger a \exp(\tilde{\mathcal{A}}t)a^\dagger|0\rangle$ are thus the probability that the process has generated N particles weighted by N. To sum over all states, we further need the projection state

$$\langle \maltese | = \sum_{N=0}^{\infty} \langle N | = \sum_{N=0}^{\infty} \frac{1}{N!} \langle 0 | a^N = \langle 0 | e^a. \quad (12)$$

The expected particle number at time t may thus be written as

$$\langle N(t) \rangle = \langle \maltese | a^\dagger a \, e^{\tilde{\mathcal{A}}t} a^\dagger | 0 \rangle. \quad (13)$$

More complicated observables and intermediate temporal evolution can be compiled following the same pattern [28]. To perform any calculations, the operators need to be normal ordered and then mapped to fields as suggested above, $a^\dagger \to \phi^\dagger(t) = 1 + \widetilde{\phi}(t)$ and $a \to \phi(t)$, where the time t corresponds to the total time the system has evolved for, Eq. (7). The expectation in Eq. (13) can thus be written as

$$\langle N(t) \rangle = \langle \phi^\dagger(t)\phi(t)\phi^\dagger(0) \rangle, \quad (14)$$

where $\langle \mathcal{O} \rangle$ denotes the path integral

$$\langle \mathcal{O} \rangle = \int \mathcal{D}[\widetilde{\phi}, \phi] \mathcal{O} e^{\mathcal{A}[\widetilde{\phi}, \phi]}. \quad (15)$$

The resulting expressions are most elegantly expressed in terms of Feynman diagrams [17]. The bare propagator of the field ϕ is read off from the bilinear part of the action which, in Fourier space, is

$$\langle \phi(\omega)\widetilde{\phi}(\omega') \rangle = \frac{\delta(\omega + \omega')}{-\hat{\imath}\omega + r} \,\hat{=}\, \rule{1.5cm}{0.4pt}, \quad (16)$$

where $\delta(\omega + \omega') = 2\pi\delta(\omega + \omega')$ denotes the scaled Dirac-δ function. Diagrammatically, the bare propagator is represented by a straight directed line. The directedness of the propagator reflects the causality [see Eq. (17)] of the process in the time domain as a particle has to be created before it can be annihilated but not vice versa. By convention, in our Feynman diagrams time proceeds from right to left.

Using the fact that the mass r is strictly positive for the Gaussian path integral to converge, we write the propagator in real time by Fourier transforming,

$$\langle \phi(t)\widetilde{\phi}(t') \rangle = \int_{-\infty}^{\infty} d\omega \, \frac{\delta(\omega + \omega')}{-\hat{\imath}\omega + r} e^{-\hat{\imath}\omega t} e^{-\hat{\imath}\omega' t'}$$
$$= \Theta(t - t')e^{-r(t - t')}, \quad (17)$$

where Θ is the Heaviside step function. If $r < 0$, then the integral in Eq. (17) is only convergent for $t < t'$, which violates causality and therefore yields an unphysical result. For this reason, we will assume $r > 0$ and we will take the limit $r \to 0$ where possible. Therefore, in this paper, the analytical results obtained through this field theory hold for the critical and subcritical regimes only ($r \geqslant 0$). However, in some cases we may be able to use probabilistic arguments that allow us to extend our results to the supercritical case ($r < 0$), see Sec. III B. Furthermore, we will drop the cumbersome Heaviside Θ functions, assuming suitable choices for the times, such as $t > t'$ above.

Each of the interaction terms of the form $\widetilde{\phi}^j\phi$ with $j \geqslant 2$ in the nonlinear part of the action Eq. (8) come with individual couplings q_j, Eq. (6). These are to be expanded perturbatively in. Following the canonical field-theoretic procedure [17,26,28], they are represented by (treelike) amputated

vertices such as

(18)

These vertices are *not* to be confused with the underlying branching process, because after the Doi-shift, lines are not representative of particles but of their correlations. For example, the vertex with coupling q_2 in Eq. (18) accounts for density-density correlations due to *any* branching or extinction, just like the propagator Eq. (16) accounts for all particle density due to *any* branching or extinction. After Fourier transforming, these processes are accounted for regardless of when they take place.

The directionality of the diagrams allows us to define *incoming* legs and *outgoing* legs of a vertex [17]. In the present branching process, all vertices have one incoming leg and j outgoing legs. We will refer to diagrams that are constructed solely from q_2 vertices as *binary tree diagrams*. The most basic such diagram is $\succ\!\!-$, which in real time reads

$$\langle \phi^2(t)\phi^\dagger(0)\rangle \triangleq 2\,\succ\!\!\!-^{q_2}$$

$$= 2q_2 \int đ\omega_1\,đ\omega_1'\,đ\omega_2\,đ\omega_2'\,đ\omega_3\,đ\omega_3'\,e^{-i\omega_2 t}e^{-i\omega_3 t}$$

$$\times \delta(\omega_1+\omega_2'+\omega_3')\frac{\delta(\omega_1+\omega_1')}{-i\omega_1+r}\frac{\delta(\omega_2+\omega_2')}{-i\omega_2+r}\frac{\delta(\omega_3+\omega_3')}{-i\omega_3+r}$$

$$= 2\frac{q_2}{r}e^{-rt}(1-e^{-rt}),\qquad(19)$$

where the pre-factor 2 is the combinatorial factor of this diagram.

The various observables that we calculate in the following are illustrated by numerics for two different kinds of continuous-time branching processes. First, the binary branching process with probabilities $p_0, p_2 \geqslant 0$ such that $p_0 + p_2 = 1$, and second, the branching process with geometric offspring distribution $p_k = p(1-p)^k$ with $p \in [0,1]$. The mass r, Eq. (5), and the rates of the couplings q_j, Eq. (6), are, in each case,

$$\text{(binary)}\quad r_B = s(1-2p_2),\qquad(20a)$$

$$q_{B2} = sp_2 = \frac{s-r_B}{2},\ q_{Bj} = 0 \text{ for } j \geqslant 3,$$

$$\text{(geometric)}\quad r_G = s\frac{2p-1}{p},$$

$$q_{Gj} = s\left(\frac{1-p}{p}\right)^j = s\left(1-\frac{r_G}{s}\right)^j.\qquad(20b)$$

Figure 1 shows typical trajectories for each case.

A. Moments $\langle N^n(t)\rangle$ and their universality

In the following we will calculate the moments of the number of particles $N(t)$, which can be determined using the particle number operator $a^\dagger a$, as introduced above. The nth

moment of $N(t)$ can be expressed as

$$\langle N^n(t)\rangle = \langle \maltese|(a^\dagger a)^n|\Psi(t)\rangle$$

$$= \sum_{\ell=0}^{n}\begin{Bmatrix}n\\\ell\end{Bmatrix}\langle \maltese|a^\ell|\Psi(t)\rangle$$

$$= \sum_{\ell=0}^{n}\begin{Bmatrix}n\\\ell\end{Bmatrix}\langle \phi^\ell(t)\widetilde{\phi}(0)\rangle,\qquad(21)$$

where $\begin{Bmatrix}n\\\ell\end{Bmatrix}$ denotes the Stirling number of the second kind for ℓ out of n [29]. We define the dimensionless function $\hat{g}_n(t)$ as the expectation

$$\hat{g}_n(t) = \langle \phi^n(t)\widetilde{\phi}(0)\rangle \triangleq n\,\vdots\!\!\!\bigotimes\!\!\!-,\qquad(22)$$

with $\hat{g}_0(t) = \langle \widetilde{\phi}(0)\rangle = 0$ and $\hat{g}_1(t) = \langle \phi(t)\widetilde{\phi}(0)\rangle = e^{-rt}$. The black circle in the diagram of Eq. (22) represents the sum of all possible intermediate nodes, allowing for internal lines. For instance,

$$\hat{g}_1(t) \triangleq \bigotimes\!\!\!- \ = \ -\!\!\!-,\qquad(23a)$$

$$\hat{g}_2(t) \triangleq \succ\!\!\!\bigotimes\!\!\!- \ = 2\,\succ\!\!\!-,\qquad(23b)$$

$$\hat{g}_3(t) \triangleq \succ\!\!\!\!\bigotimes\!\!\!- \ = 6\,\succ\!\!\!\!- + 12\,\succ\!\!\!\!\!-,\qquad(23c)$$

$$\hat{g}_4(t) \triangleq \succ\!\!\!\!\!\bigotimes\!\!\!- \ = 24\,\succ\!\!\!\!\!- + 48\,\succ\!\!\!\!\!\!-$$

$$+ 72\,\succ\!\!\!\!\!\!- + 24\,\succ\!\!\!\!\!- + 96\,\succ\!\!\!\!\!\!\!-,$$
(23d)

where the coefficient in front of each diagram is its symmetry factor, which is included in the representation involving the black circle, Eq. (22).

The tree diagrams follow a pattern, whereby $\hat{g}_n$ involves all $\hat{g}_m$ with $m < n$. For $n \geqslant 2$ this can be expressed as the recurrence relation

$$\hat{g}_n(t) \triangleq \sum_{k=2}^{n}\sum_{m_1,\ldots,m_k=1}\binom{n}{m_1,\ldots,m_k}\begin{Bmatrix}m_1\vdots\!\bigotimes\\m_2\vdots\!\bigotimes\!\!\!\diagdown_{k\,\vdots}\\m_k\vdots\!\bigotimes\end{Bmatrix},$$
(24)

where $\binom{n}{m_1,\ldots,m_k}$ denotes the multinomial coefficient with the implicit constraint of $m_1 + \cdots + m_k = n$. Including $\hat{g}_1(t)$ from Eqs. (23a) and (17), this may be written as

$$\hat{g}_n(t) = \delta_{n,1}e^{-rt} + \Bigg[\sum_{k=2}^{n}q_k\sum_{m_1,\ldots,m_k}\binom{n}{m_1,\ldots,m_k}$$

$$\times \int_0^t dt'\,e^{-r(t-t')}\hat{g}_{m_1}(t')\hat{g}_{m_2}(t')\cdots\hat{g}_{m_k}(t')\Bigg],\qquad(25)$$

where the integral accounts for the propagation up until time $t - t' \in [0,t]$ when a branching into (at least) k particles takes

place, each of which will branch into (at least) m_k particles at some later time within $[t - t', t]$.

We proceed by determining the leading order behavior of $\hat{g}_n$ in small r, starting with a dimensional argument. Since

$$\langle N^n(t) \rangle = \sum_{\ell=0}^{n} \begin{Bmatrix} n \\ \ell \end{Bmatrix} \hat{g}_\ell(t) \tag{26}$$

from Eqs. (21) and (22), $\langle N^n(t) \rangle$ being dimensionless implies the same for $\hat{g}_n(t)$. Our notation for the latter obscures the fact that $\hat{g}_n(t)$ is also a function of r and all q_j, which, by virtue of s, are rates and thus have the inverse dimension of t. We may therefore write

$$\hat{g}_n(t) = \overline{g}_n(rt; \overline{q}_2, \overline{q}_3, \ldots), \tag{27}$$

where $\overline{q}_j = q_j/r$ are dimensionless couplings. Dividing q_j by *any* rate renders the result dimensionless, but only the particular choice of dividing by r ensures that all couplings only ever enter multiplicatively (and never as an inverse), thereby enabling us to extract the asymptote of $\hat{g}_n(t)$ in the limit of small r, as we will see in the following.

Writing Eq. (25) as

$$\overline{g}_n(y; \overline{q}_2, \overline{q}_3, \ldots)$$
$$= \delta_{n,1} e^{-y}$$
$$+ \left[\sum_{k=2}^{n} \overline{q}_k \sum_{m_1, \ldots, m_k} \binom{n}{m_1, \ldots, m_k} \int_0^y dy' \, e^{-(y-y')} \right.$$
$$\left. \times \overline{g}_{m_1}(y'; \overline{q}_2, \ldots) \overline{g}_{m_2}(y'; \ldots) \cdots \overline{g}_{m_k}(y'; \ldots) \right], \tag{28}$$

the dominant terms in small r and fixed $y = rt$ are those that contain products involving the largest number of factors of $\overline{q}_j \propto r^{-1}$. Since each $\overline{q}_j$ corresponds to a branching, diagrammatically these terms are those that contain the largest number of vertices, i.e., those that are entirely made up of binary branching vertices q_2. This coupling, $q_2 = \langle \kappa(\kappa-1) \rangle/2$, cannot possibly vanish if there is any branching taking place at all. From Eqs. (27) and (28), it follows that $\hat{g}_n(t) \propto (q_2/r)^{(n-1)}$ to leading order in small r at fixed $y = rt$. Terms of that order are due to binary tree diagrams, whose contribution we denote by $g_n(t)$ in the following. For instance, $g_1(t) = \hat{g}_1(t)$, $g_2(t) = \hat{g}_2(t)$,

$$g_3(t) \,\hat{=}\, 12 \;\text{⟩—⟨} , \tag{29a}$$

$$g_4(t) \,\hat{=}\, 24 \;\text{⟨⟩—} + 96 \;\text{⟩—⟨} . \tag{29b}$$

To summarize, $\hat{g}_n(t)$ *is dominated by those terms that correspond to binary tree diagrams*, which are the trees g_n that have the largest number of vertices for any fixed n, i.e.,

$$\langle \phi^n(t) \widetilde{\phi}(0) \rangle = \hat{g}_n(t) = g_n(t) + \mathcal{O}[(1 - \langle \kappa \rangle)^{-(n-2)}], \tag{30}$$

where the correction in fact vanishes for $n < 3$.

As far as the asymptote in small r is concerned, we may thus replace $\hat{g}_\ell$ in Eq. (26) by g_ℓ. Among the $\hat{g}_\ell \sim r^{-(\ell-1)}$

with $\ell = 0, 1, , \ldots, n$, the dominating term is g_n so that the nth moment of the particle number N is, to leading order,

$$\langle N^n(t) \rangle \simeq g_n(t), \tag{31}$$

although exact results, as shown in Eq. (A1a), are easily derived using Eqs. (21), (22), (23), and (25). On the basis of Eq. (25) the recurrence relation of g_n is give by

$$g_n(t) = \delta_{n,1} e^{-rt} + q_2 \sum_{m=1}^{n-1} \binom{n}{m} \int_0^t dt' e^{-r(t-t')} g_m(t') g_{n-m}(t'), \tag{32}$$

whose exact solution is

$$g_n(t) = n! e^{-rt} \left[\frac{q_2}{r} (1 - e^{-rt}) \right]^{n-1}. \tag{33}$$

We draw two main conclusions from our results. First, that near the critical point $r = 0$, the branching process is solely characterized by the two parameters r and q_2. We therefore conclude that this process displays *universality*, in the sense that its asymptotia is exactly the same for any given r and q_2 regardless of the underlying offspring distribution. In particular, certain ratios of the moments of the particle number are universal constants (they do not depend on any parameters nor variables). For $k, \ell \in \mathbb{N}$ and $m \in 0, \ldots, k-1$, we find the constant ratios

$$\frac{\langle N^k(t) \rangle \langle N^\ell(t) \rangle}{\langle N^{k-m}(t) \rangle \langle N^{\ell+m} \rangle} = \frac{k! \ell!}{(k-m)!(\ell+m)!}. \tag{34}$$

Second, our results show that the scaling form of the moments is

$$\langle N^n(t) \rangle \simeq (q_2 t)^{n-1} \mathcal{G}_n(rt), \tag{35}$$

where $\mathcal{G}_n$ is the scaling function

$$\mathcal{G}_n(y) = n! e^{-y} \left(\frac{1 - e^{-y}}{y} \right)^{n-1}, \tag{36}$$

and the argument $y = rt$ is the rescaled time, Fig. 2. The asymptotes of $\mathcal{G}_n(y)$ characterize the behavior of the branching process in each regime,

$$\mathcal{G}_n(y) \simeq \begin{cases} n! & \text{for } y = 0, \\ n! \, y^{-(n-1)} e^{-y} & \text{for } y \to \infty. \end{cases} \tag{37}$$

Moreover, from Eq. (35), we find that the moment generating function $\mathcal{M}_N(z) = \langle e^{Nz} \rangle$ is

$$\mathcal{M}_N(z) \simeq 1 + \frac{z e^{-rt}}{1 + z \frac{q_2}{r} (e^{-rt} - 1)}. \tag{38}$$

B. Probability distribution of $N(t)$, probability of survival $P_s(t)$, and expected avalanche duration $\langle T \rangle$

Using Eq. (21) and the identity [30] of Stirling numbers of the second kind, we deduce that the falling factorial moments of $N(t)$ are

$$\langle \phi^\ell(t) \widetilde{\phi}(0) \rangle = \langle N(t)(N(t) - 1) \ldots (N(t) - \ell + 1) \rangle. \tag{39}$$

Therefore, the probability generating function of $N(t)$ is

$$\mathcal{P}_{N(t)}(z) = \sum_{\ell=0}^{\infty} \langle N(t)(N(t) - 1) \ldots (N(t) - \ell + 1) \rangle \frac{(z-1)^\ell}{\ell!}$$
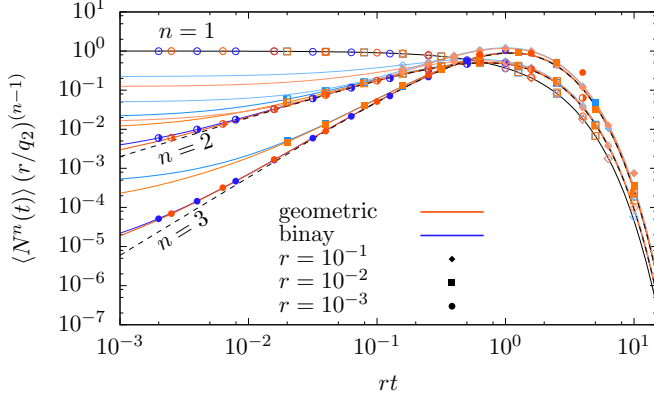
FIG. 2. Data collapse of the moments $\langle N(t)\rangle$, $\langle N^2(t)\rangle$, and $\langle N^3(t)\rangle$, as a function of rescaled time rt as of Eq. (35). Symbols show results for the binary branching process (blue) and the branching process with geometric distribution of offspring (orange), both with $r \in \{10^{-3}, 10^{-2}, 10^{-1}\}$ and $s = 1$. Solid lines indicate the exact solution in Eq. (A1a) and dashed lines indicate our approximation in Eq. (31).

$$= \sum_{\ell=0}^{\infty} \langle \phi^\ell(t)\widetilde{\phi}(0)\rangle \frac{(z-1)^\ell}{\ell!}, \tag{40}$$

and the probability distribution of $N(t)$ is, using Eqs. (30) and (33),

$$
\begin{aligned}
P(N,t) &= \frac{1}{N!}\frac{d^N}{dz^N}\left(\mathcal{P}_{N(t)}(z)\right)\big|_{z=0} \\
&\simeq \sum_{\ell=N}^{\infty}\binom{\ell}{N}\frac{(-1)^{\ell-N}}{\ell!}g_\ell(t) \\
&= \begin{cases} 1 - \frac{e^{-rt}}{1+\frac{q_2}{r}(1-e^{-rt})} & \text{if } N = 0, \\[2ex] \frac{e^{-rt}\left(\frac{q_2}{r}(1-e^{-rt})\right)^{N-1}}{\left(1+\frac{q_2}{r}(1-e^{-rt})\right)^{N+1}} & \text{if } N > 0, \end{cases}
\end{aligned}
\tag{41}
$$

which satisfies the initial condition $P(N,0) = \delta_{N,1}$ and is an exact result for binary branching processes, consistent with Ref. [13].

It is straightforward to check that Eq. (41) satisfies the master equation, Eq. (1), and the initial condition in the binary branching case. Due to the uniqueness of solutions of a system of coupled linear ordinary differential equations, the solution in Eq. (41) is the only solution. In particular, this solution holds in the supercritical case, $r < 0$. Reconstructing back the path that has lead us here, we find that $g_\ell(t)$ *is the ℓth falling factorial moment of $N(t)$*, $\langle N(t)(N(t)-1)\dots(N(t)-\ell+1)\rangle$, for binary branching processes including the supercritical case and, therefore, most expressions derived from $g_\ell(t)$ can be extended to $r < 0$. In what follows, we will specify which expressions hold in the supercritical case.

The probability of survival $P_s(t)$ is the probability that there is at least one particle at time t, i.e., $P_s(t) = P(N(t) \geqslant 1)$. Therefore, from Eq. (41),

$$P_s(t) = 1 - P(0,t) = \frac{e^{-rt}}{1+\frac{q_2}{r}(1-e^{-rt})}, \tag{42}$$
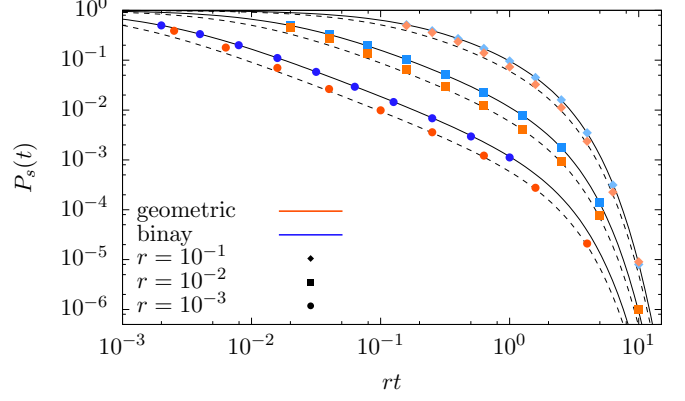

FIG. 3. Probability of survival as a function of rescaled time rt as of Eq. (42). Symbols show numerical results for the binary branching process (blue) and the branching process with geometric distribution of offspring (orange), both with $r \in \{10^{-3}, 10^{-2}, 10^{-1}\}$ and $s = 1$. Lines indicate the result in Eq. (42), which is exact for binary branching (solid lines) and approximate otherwise (dashed lines). As r gets closer to the critical value, $r = 0$, the curves $P_s(t)$ flatten and resemble the power law in Eq. (43), which has exponent -1.

and at the critical point,

$$\lim_{r\to 0} P_s(t) \simeq \frac{1}{1+q_2 t}, \tag{43}$$

which is consistent with [31–33], Fig. 3.

We define the avalanche duration T as the exact time where an avalanche dies, i.e., the time t when the process reaches the absorbing state, $T = \min\{t|N(t)=0\}$. The probability of survival $P_s(t)$ gives the probability that $T > t$. Thus, $1 - P_s(t)$ is the cumulative distribution function of the time of death and its probability density function is

$$\mathcal{P}_T(t) = -\frac{dP_s(t)}{dt} \simeq \frac{re^{rt}\left(1+\frac{q_2}{r}\right)}{\left[\frac{q_2}{r} - e^{rt}\left(1+\frac{q_2}{r}\right)\right]^2}, \tag{44}$$

and at the critical point,

$$\lim_{r\to 0}\mathcal{P}_T(t) \simeq \frac{q_2}{(1+q_2 t)^2}, \tag{45}$$

see Fig. 4. It follows from Eq. (44) that the expected avalanche duration is

$$\langle T\rangle \simeq \frac{1}{q_2}\log\left(1+\frac{q_2}{r}\right). \tag{46}$$

Because the derivation of Eq. (44) relies on a finite termination time, we cannot assume that it remains valid in the supercritical case, and similarly for Eq. (46).

C. Avalanche shape $V(t,T)$

The avalanche shape $V(t,T)$ is defined as the average of the temporal profiles $N(t)$ conditioned to extinction at
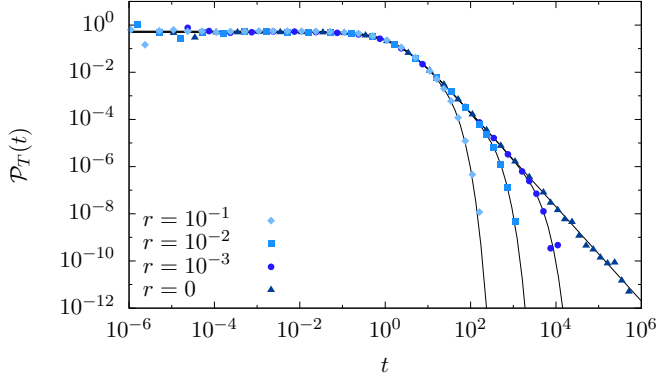
FIG. 4. Probability density function of the avalanche duration $\mathcal{P}_T(t)$ for the binary branching process with $r \in \{0, 10^{-3}, 10^{-2}, 10^{-1}\}$ and $s = 1$. Solid lines represent our result in Eqs. (44) and (45), which is exact for binary branching. Symbols show numerical results.

time T [4,34–39]. Closed form expressions of the avalanche shape have been calculated in other models such as avalanches in elastic interfaces [34], the Barkhausen noise [36], the discrete-time Ornstein-Uhlenbeck process [37]. An implicit expression of avalanche shape of branching processes is given in Ref. [4].

To produce an explicit expression we first calculate the expected number of particles at time t of a branching process conditioned to being extinct by time T, $\langle N(t)|N(T) = 0\rangle$. In terms of ladder operators,

$$\langle N(t)|N(T) = 0\rangle = \langle 0|e^{\hat{A}(T-t)}a^\dagger a e^{\hat{A}t}a^\dagger|0\rangle, \quad (47)$$

which means that a particle is created from the vacuum, the system is allowed to evolve for time t, the number of particles is measured, and the system evolves further for time $T - t$. Finally, all possible trajectories are "sieved" so that only those avalanches are whose number of particles is 0 at time T taken into account. The path integral expression of Eq. (47) is

$$\langle N(t)|N(T) = 0\rangle = \langle e^{-\phi(T)}\phi^\dagger(t)\phi(t)\phi^\dagger(0)\rangle$$
$$= \langle \phi(t)\widetilde{\phi}(0)\rangle + \sum_{n \geqslant 1}\frac{(-1)^n}{n!}$$
$$\times (\langle \phi^n(T)\phi(t)\widetilde{\phi}(0)\rangle$$
$$+ \langle \phi^n(T)\widetilde{\phi}(t)\phi(t)\widetilde{\phi}(0)\rangle). \quad (48)$$

The two terms in the bracket have asymptotes

$$\langle \phi^n(T)\phi(t)\widetilde{\phi}(0)\rangle \simeq \sum_{k=1}^{n}\sum_{m_1,\dots,m_k}\binom{n}{m_1,\dots,m_k}\frac{1}{k!}$$
$$\times g_{m_1}(T-t)\cdots g_{m_k}(T-t)g_{k+1}(t), \quad (49)$$

and

$$\langle \phi^n(T)\widetilde{\phi}(t)\phi(t)\widetilde{\phi}(0)\rangle \simeq \sum_{k=1}^{n}\sum_{m_1,\dots,m_k}\binom{n}{m_1,\dots,m_k}\frac{1}{(k-1)!}$$
$$\times g_{m_1}(T-t)\cdots g_{m_k}(T-t)g_k(t), \quad (50)$$

with the constraint $m_1 + \cdots + m_k = n$ in both cases. Both expressions are exact in case of binary branching. Their diagrammatic representation and closed form expressions can be found in Appendix B. Using the expression of $g_n(t)$ in Eq. (33) and the number of combinations of n legs into k groups, we have

$$\langle N(t)|N(T) = 0\rangle$$
$$= e^{-rt} - P_s(T)\left[1 + \frac{q_2}{r}(1 - e^{-rt})\left(2 - \frac{P_s(T)}{P_s(t)}\right)\right], \quad (51)$$

where $P_s(t)$ is given in Eq. (42).

To account solely for those instances that become extinct exactly at time T, the expectation $\langle N(t)|N(T) = 0\rangle$ is to be differentiated with respect to T, and to account for the factor due to conditioning to extinction, we need to divide the result by $-\frac{d}{dt}P_s(t)$, yielding,

$$V(t, T) = \frac{\frac{d}{dT}\langle N(t)|N(T) = 0\rangle}{-\frac{d}{dt}P_s(t)}$$
$$\simeq 1 + 2\frac{q_2}{r}(1 - e^{-rt})\left[1 - \frac{P_s(T)}{P_s(t)}\right], \quad (52)$$

Fig. 5(a). Since the observable $V(t, T)$ suitably incorporates the condition $N(T) = 0$, the result in Eq. (52) holds for the supercritical case as well. At criticality, the avalanche shape is the parabola [4,36–38]

$$\lim_{r \to 0} V(t, T) \simeq 1 + 2\frac{(q_2 T)^2}{1 + q_2 T}\left(1 - \frac{t}{T}\right)\frac{t}{T}. \quad (53)$$

The avalanche shape $V(t, T)$ in Eq. (52) is a symmetric function with its maximum at $t = T/2$, which is bounded [37] by

$$\lim_{T \to \infty} V\left(\frac{T}{2}, T\right) \simeq 1 + 2\frac{q_2}{r}. \quad (54)$$

D. Connected correlation function Cov$(N(t_1), N(t_2))$

To calculate the expectation $\langle N(t_1)N(t_2)\rangle$ we assume $0 < t_1 < t_2$ without loss of generality,

$$\langle N(t_1)N(t_2)\rangle = \langle \maltese|a^\dagger a e^{-\hat{A}(t_2 - t_1)}a^\dagger a e^{-\hat{A}t_1}a^\dagger|0\rangle \quad (55a)$$
$$= \langle \phi(t_2)\phi^\dagger(t_1)\phi(t_1)\phi^\dagger(0)\rangle \quad (55b)$$
$$= \langle \phi(t_2)\widetilde{\phi}(t_1)\phi(t_1)\widetilde{\phi}(0)\rangle + \langle \phi(t_2)\phi(t_1)\widetilde{\phi}(0)\rangle \quad (55c)$$
$$\hat{=} \quad \text{———} \quad \text{———} \quad + 2 \quad \text{>——} \quad (55c)$$

The diagram on the left consists of two separate components. We refer to diagrams of that kind as disconnected diagrams, in contrast to connected diagrams that only consist of one component as the one appearing on the right. The connected correlation function is

$$\text{Cov}(N(t_1), N(t_2)) = \langle N(t_1)N(t_2)\rangle - \langle N(t_1)\rangle\langle N(t_2)\rangle$$
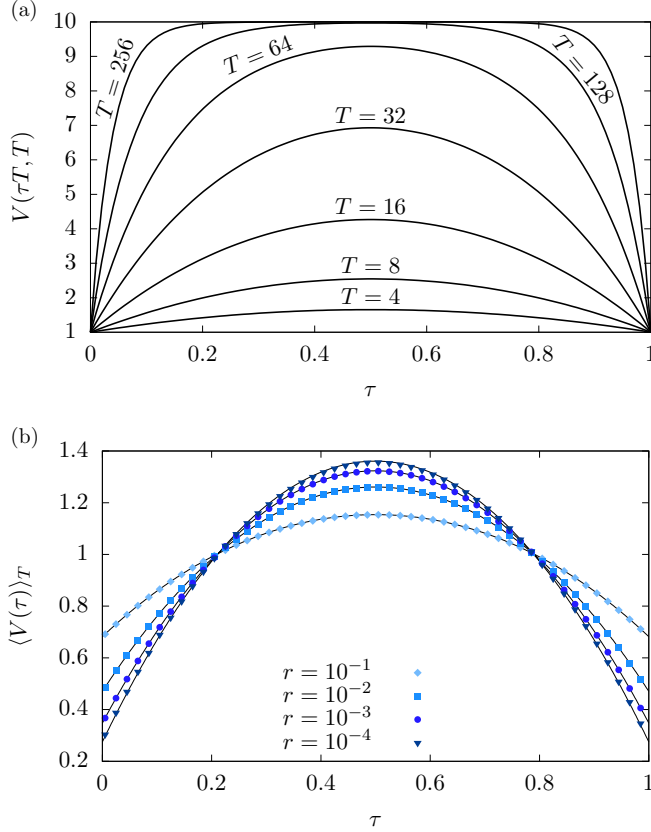$$= \left(2\frac{q_2}{r} + 1\right)e^{-r(t_1 + t_2)}(e^{rt_1} - 1), \quad (56)$$

(a)

(b)

FIG. 5. In (a), avalanche shape V with rescaled time $\tau = t/T$ for different times of extinction T, $r = 10^{-1}$ and $q_2 = 0.45$ as of Eq. (52). The shapes are symmetric and flatten as T increases with the upper bound given in Eq. (54). However, this observable is numerically unaccessible because it is computationally unfeasible to obtain a large enough sample of avalanches in the subcritical regime conditioned to extinction at large times. Instead, in (b) we show an observable that is accessible both numerically and analytically, the averaged avalanche shape $\langle V(\tau) \rangle_T$, that is for each r, avalanches are rescaled in time to the interval $[0,1]$, their shapes are averaged and normalised regardless of their extinction times T. Numerical results shown as symbols are for the binary branching process with $r \in \{10^{-4}, 10^{-3}, 10^{-2}, 10^{-1}\}$ and $s = 1$, and are in agreement with Eq. (C2) (solid lines), which is an exact expression for binary branching processes. We find that the shape tends to a parabola as r approaches the critical point.

which is an exact result independent of the type of branching process, (i.e., irrespective of the offspring distribution), Fig. 6. In particular, the variance is $\mathrm{Var}(N(t)) = \mathrm{Cov}(N(t), N(t))$ [17].

E. *n*-point correlation function

We call $\zeta_n(t_1, \ldots, t_n)$, with $0 < t_1, \ldots, t_n$ (not necessarily in order), the contribution of all binary, and therefore connected, diagrams to the *n*-point correlation function, where the error term is controlled as

$$\langle N(t_1) \ldots N(t_n) \rangle = \zeta_n(t_1, \ldots, t_n) + \mathcal{O}((1 - \langle \kappa \rangle)^{-(n-2)}).$$
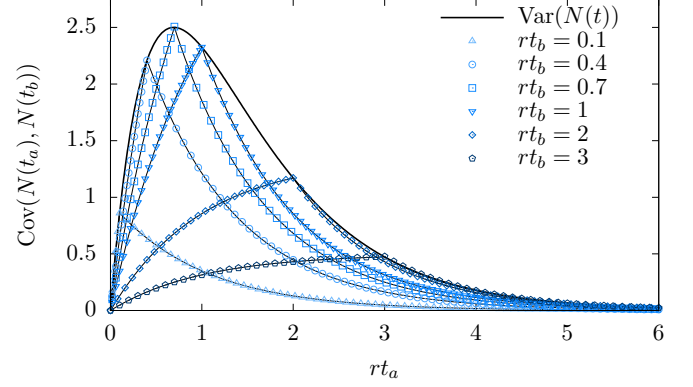
(57)

FIG. 6. Two-point correlation function $\mathrm{Cov}(N(t_a), N(t_b))$ of the binary continuous-time branching process with $r = 10^{-1}$ and $s = 1$. Our numerical results shown as symbols are in perfect agreement with the exact expression in Eq. (56) with $t_1 = \min(t_a, t_b)$ and $t_2 = \max(t_a, t_b)$ (solid lines). We also show $\mathrm{Var}(N(t)) = \mathrm{Cov}(N(t), N(t))$, which is the envelope.

The leading order contribution ζ_n satisfies the following recurrence relation,

$$\zeta_n(t_1, \ldots, t_n) \tag{58a}$$

$$= \sum_{m=1}^{n-1} \sum_{\substack{\sigma \subset \{t_1, \ldots, t_n\} \\ |\sigma| = m}} \left\{ \quad \right\} \tag{58b}$$

$$= q_2 \sum_{m=1}^{n-1} \sum_{\substack{\sigma \subset \{t_1, \ldots, t_n\} \\ |\sigma| = m}} \int_0^{t_{\min}} \zeta_m(t_{\sigma(1)} - t', \ldots, t_{\sigma(m)} - t')$$

$$\times \zeta_{n-m}(t_{\sigma^c(m+1)} - t', \ldots, t_{\sigma^c(n)} - t')e^{-rt'}dt', \tag{58c}$$

with $\zeta_0 = 0$ and $\zeta_1(t) = e^{-rt}$, and $t_{\min} = \min\{t_1, \ldots, t_n\}$. Here, σ is a subset of the set of times $\{t_1, \ldots, t_n\}$, whose size is $|\sigma|$, and $\sigma(1), \ldots, \sigma(m)$ is a list of its distinct elements. Its complementary set is $\sigma^c = \{t_1, \ldots, t_n\} \backslash \sigma$, which contains the elements $\sigma^c(m+1), \ldots, \sigma^c(n)$. Equation (58) is symmetric under exchange of any permutation of the times $t_1, \ldots, t_n$, see the three-point correlation function in Appendix A.

This approximation is twofold. First, it neglects higher order branching vertices proportional to $q_{j \geqslant 3}$, and second, it neglects contributions from disconnected diagrams, cf. Eq. (55). Latter contributions are dominant only when $t_{\max} = \max\{t_1, \ldots, t_n\}$ is smaller than s^{-1}. For times in $(0, s^{-1})$, the branching process has typically not yet undergone a change in the particle number.

F. Distribution of the total avalanche size *S*

We define the total avalanche size as the time-integrated activity $S = s \int dt N(t)$. Using $\langle N(t) \rangle = e^{-rt}$ and Eq. (56), the first and second moments of the total avalanche size [8,40]
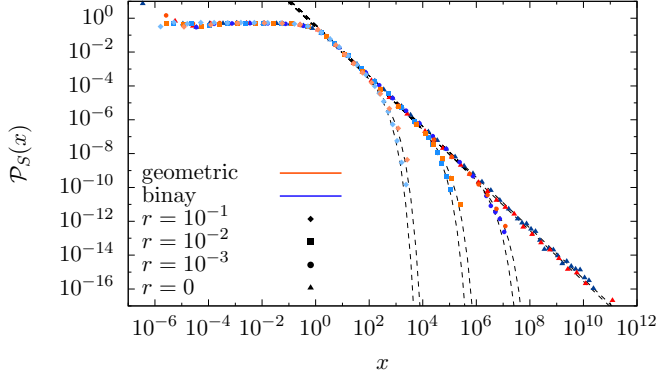
FIG. 7. Probability density function of the total avalanche size $\mathcal{P}_S(x)$ for the binary branching process (blue) and the branching process with geometric distribution of offspring (orange), with $r \in \{0, 10^{-3}, 10^{-2}, 10^{-1}\}$ and $s = 1$. Dashed lines indicate our approximation in Eq. (63). This approximation is not valid for small times, which explains the disagreement between the numerical results and the dashed lines for small values of x.

read

$$\langle S \rangle = s \int dt \langle N(t) \rangle = \frac{s}{r} = \frac{1}{1 - \langle \kappa \rangle}, \qquad (59a)$$

$$\langle S^2 \rangle = s^2 \int dt_1 dt_2 \langle N(t_1)N(t_2) \rangle = \frac{s^2}{r^2}\left(\frac{q_2}{r} + 1\right). \qquad (59b)$$

To calculate $\langle S^n \rangle$ close to criticality, we use the approximation to the n-point correlation function defined in Eq. (57) and find the following recurrence relation,

$$\langle S^n \rangle \simeq s^n \int dt_1 \ldots dt_n \, \zeta_n(t_1, \ldots, t_n)$$

$$\simeq \frac{q_2}{r} \sum_{m=1}^{n-1} \binom{n}{m} \langle S^m \rangle \langle S^{n-m} \rangle$$

$$\simeq \frac{s^n q_2^{n-1}}{r^{2n-1}} 2^{n-1}(2n - 3)!!, \qquad (60)$$

see Appendix D for a proof by induction of Eq. (60). Similar to Eq. (34), we find the universal constant ratios of the moments of S,

$$\frac{\langle S^k \rangle \langle S^\ell \rangle}{\langle S^{k-m} \rangle \langle S^{\ell+m} \rangle} = \frac{(2k-3)!!(2\ell-3)!!}{(2(k-m)-3)!!(2(\ell+m)-3)!!}, \quad (61)$$

with $k, \ell \in \mathbb{N}$ and $m \in \{0, \ldots, k-1\}$. The moment generating function of S is

$$\mathcal{M}_S(z) \simeq 1 + \frac{r - \sqrt{r^2 - 4sq_2z}}{2q_2}, \qquad (62)$$

and its probability density function $\mathcal{P}_S(x)$ is the inverse Laplace transform of $\mathcal{M}_S(-z)$,

$$\mathcal{P}_S(x) \simeq \frac{1}{2}\sqrt{\frac{s}{q_2\pi}} x^{-\frac{3}{2}} e^{-\frac{r^2x}{4q_2s}}, \qquad (63)$$

which is a power law with exponent $-3/2$ with exponential decay, Fig. 7. At criticality, this distribution is a pure power law.

The approximation used to derive these results, Eq. (57), consists in neglecting contributions of disconnected diagrams to the n-point correlation function. This approximation is unjustified for total avalanche sizes corresponding those realisations of branching processes that underwent no branching but a single extinction event, and whose sizes are therefore typically smaller than 1, because their n-point correlation functions $\langle N(t_1) \ldots N(t_n) \rangle$ vanish for $t_{\max} \gtrsim s^{-1}$. Consequently, the n-point correlation functions are dominated by purely disconnected diagrams (cf. Sec. III E). We therefore expect a breakdown of our approximation around $x = 1$. All three features of the distribution of the total avalanche size, the power-law behavior, the exponential cutoff, and the breakdown of the approximation for $x < 1$, are in good agreement with numerical simulations as shown in Fig. 7.

IV. DISCUSSION AND CONCLUSIONS

In this paper we study the continuous-time branching process following a field-theoretic approach. We build on the wealth of existing results in the literature obtained through other methods. Here, we demonstrate that the Doi-Peliti field theory provides an elegant, intuitive, and seemingly natural language for continuous-time branching processes.

We illustrate how to use the field theory to calculate a number of relevant observables, listed in Table I. Our results are valid for any offspring distribution in the vicinity of the critical point and at large times. However, many of the results are exact for the binary branching process and others are exact for any branching process. In principle, many observables can be calculated systematically using the field theory for any offspring distribution, for any time and any parameter set.

In this paper, we extend the existing results in the literature by finding explicit scaling functions and universal moment ratios for any offspring distribution. We find that all the scaling laws derived above depend on two parameters only, namely r and q_2. Therefore, one may argue that the master equation of any branching process close to the critical point and asymptotically in large times is captured by the action Eq. (8) with couplings r and q_2 only.

Having established the field-theoretic ground work, in particular the basic formalism and range of relevant observables, we may now proceed by extending the basic branching process into more sophisticated models of natural phenomena. We hope that the methods established in this paper will help reaching new boughs, branches, and twigs of the many offspring of branching processes.

APPENDIX A: EXACT EXPRESSIONS

The continuous-time branching process is exactly solvable, that is, in principle, all moments and correlation functions can

be calculated in exact form if all the terms in the (possibly infinite) sums are taken into account. Here we show some exact expressions. The exact first three moments of $N(t)$ are

$$\langle N(t) \rangle = e^{-rt}, \tag{A1a}$$

$$\langle N^2(t) \rangle = e^{-rt}\left[1 + \frac{2q_2}{r}(1 - e^{-rt})\right], \tag{A1b}$$

$$\langle N^3(t) \rangle = e^{-3rt}\left(\frac{6q_2^2}{r^2} - \frac{3q_3}{r}\right) - e^{-2rt}\left(\frac{12q_2^2}{r^2} + \frac{6q_2}{r}\right)$$
$$+ e^{-rt}\left(\frac{6q_2^2}{r^2} + \frac{3q_3}{r} + \frac{6q_2}{r} + 1\right), \tag{A1c}$$

and therefore the variance is

$$\text{Var}(N(t)) = \left(1 + 2\frac{q_2}{r}\right)e^{-rt}(1 - e^{-rt}), \tag{A2}$$

which is consistent with Eq. (56) and [1,13,17,27,32]. The three-point correlation function is, assuming $0 \leqslant t_1 \leqslant t_2 \leqslant t_3$ and using Eq. (58c),

$$\langle N(t_1)N(t_2)N(t_3) \rangle \simeq \zeta(t_1, t_2, t_3)$$
$$= 2\left(\frac{q_2}{r}\right)^2 e^{-r(t_1+t_2+t_3)}$$
$$\times \left[(e^{rt_1} - 1)(2e^{rt_1} + e^{rt_2}) - \frac{3}{2}(e^{2rt_1} - 1)\right]. \tag{A3}$$

APPENDIX B: DIAGRAMMATIC REPRESENTATION AND CLOSED FORM EXPRESSIONS OF Eqs. (49) AND (50)

Defining

$$a = \frac{e^{-r(T-t)} - e^{-rT}}{1 - e^{-r(T-t)}}, \tag{B1}$$

we have, first, Eq. (49),

$$\langle \phi^n(T)\phi(t)\widetilde{\phi}(0) \rangle$$
$$= \sum_{k=1}^{n} \sum_{m_1,\ldots,m_k} \binom{n}{m_1,\ldots,m_k}$$
$$\times g_{m_1}(T-t)\cdots g_{m_k}(T-t)g_{k+1}(t)\frac{1}{k!} \tag{B2a}$$

$$\hat{=} \sum_{k=1}^{n} \sum_{m_1,\ldots,m_k} \binom{n}{m_1,\ldots,m_k} \left\{ \begin{array}{c} \text{diagram} \end{array} \right\}$$

$$= n!e^{-rt}\left(\frac{q_2}{r}\right)^n (1 - e^{-rT})^n \left[\frac{a^2(n-1)}{(1+a)^2} + \frac{2a}{1+a}\right], \tag{B2b}$$

and second, Eq. (50),

$$\langle \phi^n(T)\widetilde{\phi}(t)\phi(t)\widetilde{\phi}(0) \rangle$$
$$= \sum_{k=1}^{n} \sum_{m_1,\ldots,m_k} \binom{n}{m_1,\ldots,m_k}$$
$$\times g_{m_1}(T-t)\cdots g_{m_k}(T-t)g_k(t)\frac{1}{(k-1)!} \tag{B3a}$$

$$\hat{=} \sum_{k=1}^{n} \sum_{m_1,\ldots,m_k} \binom{n}{m_1,\ldots,m_k} \left\{ \begin{array}{c} \text{diagram} \end{array} \right\}$$

$$= \frac{n!e^{-rt}}{1-e^{-rt}}\left(\frac{q_2}{r}\right)^{n-1}(1 - e^{-rT})^n \left[\frac{a^2(n-1)}{(1+a)^2} + \frac{a}{1+a}\right]. \tag{B3b}$$

APPENDIX C: AVERAGED AVALANCHE SHAPE

In Sec. III C, we derive analytically the expected avalanche shape $V(t, T)$ for a specific time of death T. However, direct comparison with numerics is computationally very expensive as specific large times of death occur rarely for subcritical branching processes. Here we describe an observable that is accessible both analytically and numerically: the averaged avalanche shape $\langle V(\tau) \rangle_T$. For a fixed parameter set, we first rescale time $\tau = t/T$ and then average all the avalanche profiles irrespectively of T. Finally, to achieve convergence to a shape comparable across parameter settings, we normalise the result by area [38],

$$\langle V(\tau) \rangle_T = \frac{1}{N_V} \int_0^\infty dT \mathcal{P}_T(T) V(\tau T, T), \tag{C1a}$$

$$N_V = \int_0^1 \int_0^\infty d\tau dT \mathcal{P}_T(T) V(\tau T, T). \tag{C1b}$$

The result [41] can be expressed with the Gaussian hypergeometric function $_2F_1(a, b, c, z)$,

$$\langle V(\tau) \rangle_T = \frac{1}{N_V} + \tau(\tau - 1)\frac{q_2 F(\tau, q_2, r)}{(q_2 + r)N_V}, \tag{C2}$$

where

$$F(\tau, q_2, r) = \frac{_2F_1\left(1, 2-\tau, 3-\tau, \frac{q_2}{q_2+r}\right)}{\tau - 2}$$
$$- \frac{_2F_1\left(1, 1+\tau, 2+\tau, \frac{q_2}{q_2+r}\right)}{\tau + 1}. \tag{C3}$$

Both F and N_V diverge at the critical point with the limit

$$\lim_{r \to 0} \frac{F(\tau, q_2, r)}{N_V} = 6. \tag{C4}$$

APPENDIX D: PROOF OF Eq. (60)

Equation (60) can be proved by induction. In Eq. (59) we see that it applies to $\langle S \rangle$. The approximation of binary tree diagrams of $\langle N(t_1)N(t_2) \rangle$ gives $\langle S^2 \rangle = s^2 q_2/r^3$, which also satisfies Eq. (60). The induction step is verified by

$$\langle S^n \rangle = \frac{q_2}{r} \sum_{m=1}^{n-1} \binom{n}{m} \left(\frac{s^m q_2^{m-1} 2^{m-1}(2m-3)!!}{r^{2m-1}}\right)$$
$$\times \left(\frac{s^{n-m} q_2^{n-m-1} 2^{n-m-1}(2(n-m)-3)!!}{r^{2(n-m)-1}}\right)$$

$$= \frac{s^n q_2^{n-1}}{r^{2n-1}} 2^{n-2} \sum_{m=1}^{n-1} \binom{n}{m}(2m-3)!!(2(n-m)-3)!!.$$

$$\text{(D1)}$$

This sum is equivalent to

$$\sum_{m=1}^{n-1} \binom{n}{m}(2m-3)!!(2(n-m)-3)!! \qquad \text{(D2a)}$$

$$= \frac{1}{n-1} \sum_{m=1}^{n-1} \binom{n}{m}(2m-3)!!(2(n-m)-1)!!$$

$$= \frac{1}{n-1} \sum_{k=0}^{n-2} \binom{n}{k+1}(2k-1)!!(2(n-k)-3)!!$$

$$= 2(2n-3)!!, \qquad \text{(D2b)}$$

where we have used the identity [42],

$$\sum_{k=0}^{n-1} \binom{n}{k+1}(2k-1)!!(2(n-k)-3)!! = (2n-1)!!.$$

$$\text{(D3)}$$

Using Eq. (D2) in Eq. (D1) reproduces Eq. (60), thereby completing the proof.

[1] T. E. Harris, *The Theory of Branching Processes* (Springer-Verlag, Berlin, 1963).

[2] S. Zapperi, K. B. Lauritsen, and H. E. Stanley, Phys. Rev. Lett. **75**, 4071 (1995).

[3] D. S. Lee, K. I. Goh, B. Kahng, and D. Kim, J. Korean Phys. Soc. **44**, 633 (2004).

[4] J. P. Gleeson and R. Durrett, Nat. Com. **8**, 1227 (2017).

[5] E. N. Gilbert, J. SIAM **9**, 533 (1961).

[6] R. Durrett, Random Graph Dynamics, Vol. 20 *of Cambridge Series in Statistical and Probabilistic Mathematics* (Cambridge University Press, Cambridge, 2006).

[7] W. Marzocchi and A. M. Lombardi, J. Geophys. Res. **113**, B08317 (2008).

[8] A. Corral and F. Font-Clos, in *Self-Organized Criticality Systems*, edited by M. J. Aschwanden (Open Academic Press, Berlin, 2013), pp. 183–228.

[9] W. J. Reed and B. D. Hughes, Phys. A **319**, 579 (2003).

[10] M. Kimmel and D. E. Axelrod, *Branching Processes in Biology (Interdisciplinary Applied Mathematics)*, Vol. 19 (Springer, Berlin, 2002).

[11] R. Durrett, in *Branching Process Models of Cancer* (Springer, Berlin, 2015), pp. 1–63.

[12] M. M. R. Williams, *Random Processes in Nuclear Reactors* (Elsevier, Amsterdam, 2013).

[13] I. Pázsit and L. Pál, *Neutron Fluctuations: A Treatise on the Physics of Branching Processes* (Elsevier, Amsterdam, 2007).

[14] D. N. Rockmore, C. Fang, N. J. Foti, T. Ginsburg, and D. C. Krakauer, J. Assoc. Info. Sci. Technol. **69**, 483 (2018).

[15] S. Seshadri, A. Klaus, D. E. Winkowski, P. O. Kanold, and D. Plenz, Transl. Psychiat. **8**, 3 (2018).

[16] J. M. Beggs and D. Plenz, J. Neurosci. **23**, 11167 (2003).

[17] U. C. Täuber, *Critical Dynamics* (Cambridge University Press, Cambridge, UK, 2014), pp. i–xvi,1–511.

[18] C. W. Gardiner, *Handbook of Stochastic Methods*, 2nd ed. (Springer-Verlag, Berlin, 1997).

[19] G. R. Grimmett and D. R. Stirzaker, *Probability and Random Processes*, 2nd ed. (Oxford University Press, New York, NY, 1992).

[20] L. Pal, Nuovo Cim. **7**, 25 (1958).

[21] G. I. Bell, Nucl. Sci. Engr. **21**, 390 (1965).

[22] Y. Kitamura and T. Misawa, Ann. Nucl. Energy **123**, 119 (2019).

[23] J.-F. Le Gall, Probab. Surv. **2**, 245 (2005).

[24] D. Aldous, Ann. Probab. **21**, 248 (1993).

[25] M. Doi, J. Phys. A: Math. Gen. **9**, 1465 (1976).

[26] L. Peliti, J. Phys. (Paris) **46**, 1469 (1985).

[27] R. Dickman and R. Vidigal, Braz. J. Phys. **33**, 73 (2003).

[28] U. C. Täuber, M. Howard, and B. P. Vollmayr-Lee, J. Phys. A: Math. Gen. **38**, R79 (2005).

[29] The Stirling numbers of the second kind can be calculated using the expression $\{\begin{smallmatrix} n \\ \ell \end{smallmatrix}\} = \frac{1}{\ell!} \sum_{j=0}^{\ell} (-1)^{\ell-j} \binom{\ell}{j} j^n$.

[30] The Stirling numbers of the second kind satisfy the identity $N^n = \sum_{\ell=0}^{n} \{\begin{smallmatrix} n \\ \ell \end{smallmatrix}\} N(N-1)\ldots(N-\ell+1)$.

[31] R. Garcia-Millan, F. Font-Clos, and A. Corral, Phys. Rev. E **91**, 042122 (2015).

[32] N. Wei and G. Pruessner, Phys. Rev. E **94**, 066101 (2016), comment on Ref. [31].

[33] Á. Corral, R. Garcia-Millan, and F. Font-Clos, PloS One **11**, e0161586 (2016).

[34] A. Dobrinevski, P. Le Doussal, and K. J. Wiese, Europhys. Lett. **108**, 66002 (2015).

[35] M. A. Sheikh, R. L. Weaver, and K. A. Dahmen, Phys. Rev. Lett. **117**, 261101 (2016).

[36] S. Papanikolaou, F. Bohn, R. L. Sommer, G. Durin, S. Zapperi, and J. P. Sethna, Nat. Phys. **7**, 316 (2011).

[37] A. Baldassarri, F. Colaiori, and C. Castellano, Phys. Rev. Lett. **90**, 060601 (2003).

[38] G. Willis and G. Pruessner, Int. J. Mod. Phys. **32**, 1830002 (2018).

[39] L. Laurson, X. Illa, S. Santucci, K. T. Tallakstad, K. J. Måløy, and M. J. Alava, Nat. Commun. **4**, 2927 (2013).

[40] A. Corral, R. Garcia-Millan, N. R. Moloney, and F. Font-Clos, Phys. Rev. E **97**, 062156 (2018).

[41] Wolfram Research Inc., *Mathematica* (Wolfram Research, Champaign, IL, 2018), version 11.3.0.0.

[42] D. Callan, arXiv preprint arXiv:0906.1317 (2009).